

Article

Effects of Inoculation on Structure Characteristics of High Silicon Ductile Cast Irons in Thin Wall Castings

Iulian Riposan, Eduard Stefan, Stelian Stan *, Nicoleta Roxana Pana and Mihai Chisamera

Materials Science and Engineering Faculty, Politehnica University of Bucharest, 313 Spl. Independentei, 060042 Bucharest, Romania; iulian.riposan@upb.ro (I.R.); stefan_eduard2000@yahoo.com (E.S.); pana.nicoletaroxana@yahoo.com (N.R.P.); chisameramihai@gmail.com (M.C.)

* Correspondence: constantin.stan@upb.ro; Tel.: +40-7443-98079

Received: 23 June 2020; Accepted: 9 August 2020; Published: 12 August 2020



Abstract: Previous experiments pointed out that the deviation using a sphere as reference of graphite particles is noticeably increased by Si-alloying, with inoculation as a possible beneficial effect. The main objective of the present work is to evaluate the effects of commercial inoculants (Ca/Ca, Ba/Ca, RE-FeSi alloys) on 4.5%Si ductile iron, thin wall castings. FeSiMgRE treated iron (0.032–0.036%Mg_{res}) is in-mold inoculated (a four-work-positions pattern). A complex chemical composition is obtained for each inoculation variant. Wedge casting W₃ (ASTM A 367) is used to evaluate structure characteristics at different wall thickness (3–15 mm). Minimum and maximum size, area, nodule count, and representative graphite shape factors are evaluated. Roundness (including A_G and F_{max}) at 0.6–0.8 level illustrates the common formation of slightly irregular spheroidal graphite (Type V, ISO 945). Ca, RE-FeSi inoculation leads to the highest level of real perimeter and, consequently, to the lowest level of Sphericity. Ca, Ba-FeSi inoculation appears to be better than simple Ca-FeSi for improving graphite parameters, while Ca, RE-FeSi has the lowest beneficial effect, especially as it negatively affects the compactness degree of graphite particles. A two-step liquid treatment using RE-bearing FeSiCaMg master alloy and Ca, Ba-FeSi inoculant appears to be a solution to improve graphite parameters for high-Si ductile irons solidified in thin wall castings.

Keywords: high Si ductile cast iron; thin wall casting; inoculation; in-mold; structure; graphite; Ca; Ca-Ba; Ca-RE

1. Introduction

The substitution of cast iron components with Al reduces weight in the automotive industry and it is very attractive for it improves fuel economy and reduces CO₂ emissions. Unfortunately, two important aspects of this substitution are not considered. Al production consumes significantly more energy than cast iron, both during primary manufacturing (five times higher than pig iron) and in the foundry. On the other hand, the emissions legislation in the automotive industry focuses entirely on tailpipe emissions, with no consideration for the CO₂ generated during production of the vehicle, and production, delivery, and consumption of the fuel. If the full life cycle emissions are considered, the use of cast iron in car production has to be reconsidered [1].

In order to remain competitive in the automotive industry, the iron castings must reduce their weight, so thin wall iron castings concept will sustain the survival of cast iron in this industry. It has been shown that thin wall wheel rims made of ductile iron can have the same weight and better mechanical properties than their substitutes made of aluminum alloys [2].

It is possible to produce thin wall castings (control arms, cantilevers, and rotors) made of ductile iron without the development of chills, cold laps, or misruns, and with a strength to weight ratio of up to 87 MPa·cm³·g⁻¹. In addition, austempering heat treatment promotes the development

of a fully ausferritic matrix in thin wall castings with a strength to weight ratio increase of up to $154 \text{ MPa}\cdot\text{cm}^3\cdot\text{g}^{-1}$ [3].

In cast iron, silicon promotes solid solution hardened ferrite at higher strength, hardness, and resistance to oxidation and corrosion, but at reduced elongation and toughness level. Usually, conventional (un-alloyed) cast irons contain up to 3%Si, while 3–18%Si range characterizes the Si-alloyed cast irons (High Si-cast irons). Three groups of high silicon cast irons are generally used, by capitalization of beneficial effects of silicon alloyed metal matrix [4,5]:

- (a) 3.2–4.3%Si ductile cast irons, where the un-stable mixed ferrite-pearlite matrix is replaced with more predictable and controllable ferritic grades, at reduced hardness variation, increased cutting tool life, and better mechanical properties are ($R_m = 450\text{--}650 \text{ MPa}$; $R_{p0.2} = 350\text{--}500 \text{ MPa}$; $A = 10\text{--}20\%$) usually used in automotive industry.
- (b) Si (4–6%Si) and Si-Mo (2.5–5.5%Si and 0.2–2.0%Mo) ductile cast irons, for resistance to oxidation and corrosion at high temperatures. Mo addition favors superior mechanical properties, especially at high temperatures ($R_m = 400\text{--}650 \text{ MPa}$; $R_{p0.2} = 250\text{--}550 \text{ MPa}$; $A = 3\text{--}12\%$), typically for exhausted applications.
- (c) 14–18%Si, for higher resistance to corrosion.

Silicon alloyed ductile irons (EN 1563 and ISO 1083) and Si-Mo alloyed ductile irons (SAE J 2582) occupy distinct positions comparing to the standard cast irons, such as conventional ductile irons (EN 1563, ISO 1083, and ASTM A 536), as strength and elongation relationships: a middle position as elongation level, for higher strength properties values. Supplementary Mo alloying reduces specially ductility characteristics of high silicon ductile irons [4,5].

Silicon is known as an element favoring spheroidal graphite degeneration, up to chunky graphite formation [6–8], while Ce/Sb [7] or Bi [8,9] have a beneficial effect to counteract this type of graphite. A chunky graphite-free microstructure is closely related to the acting combination of Si and trace elements, and the solidification time, which itself corresponds to the wall thickness [10].

It was found that the amount of chunky graphite can significantly be reduced by the addition of Sb. This means that the critical Si level can be increased when Sb is added. Regarding graphite particles, important amounts of degenerated shapes assigned to chunky graphite are obtained by increasing silicon levels. In a number of alloys, antimony additions are effective for decreasing the formation of chunky graphite even at silicon contents higher than 6 wt.% [11,12]. According to a paper [8], special inoculation techniques are necessary, adjusted to the high Si content and the solidification rate (time).

In a literature review, Stefanescu and Ruxanda [13] pointed out that to achieve a carbide free structure with a wall thickness less than five millimeters, one must further increase the carbon equivalent (CE) to 4.75–4.92%. When the CE reaches 5%, not only the structure will be carbide free, but also 40% ferrite will be present in the matrix. Finally, a completely ferritic structure can be obtained with $CE = 5.28\%$ (3.95%C, 4%Si). In proper experiments, it was demonstrated that carbide-free 2.5 mm-thick plates can be obtained through a two-step liquid treatment (Fe-Si-6Mg-1RE nodularization and 0.6% Fe-75Si-1Ca inoculation), with a base iron composition of 4.0% C, 2.8%Si, 0.2%Mn, 0.02%P, 0.02%S, and a pouring temperature of 1477 °C. The properties of these ductile iron thin wall castings are rather sensitive to surface quality and graphite shape. Lower properties are associated with rougher surfaces and lower graphite sphericity [13].

As inoculation is generally used in ductile iron production not only to avoid carbides formation but also to improve the nodular graphite characteristics [14], the main objective of the present work is to evaluate the effects of inoculation on high silicon content (4.5%Si) ductile iron, and to compare the behavior of the usually used commercial inoculants, such as: Ca-FeSi, Ca, Ba-FeSi, and Ca, RE-FeSi alloys in controlled in-mold inoculation conditions of thin wall castings.

2. Materials and Methods

A 10 kg-coreless induction furnace, 8000 Hz frequency is used to produce test cast irons, with high purity pig iron, ductile cast iron scrap, and ferrosilicon as charge materials. The melt is superheated to 1525 °C, held for 5 min, and tapped into a pre-heated tundish treatment ladle for nodularization treatment (1.5 wt.%FeSiCaMgRE alloy, Table 1).

An in-the-mold inoculation pattern for four-work-position is used, (Figure 1) including a central down-sprue that supplied Mg-treated iron simultaneously to four separate reaction test chambers (one as un-inoculated reference and three to test Ca-FeSi, Ca, Ba-FeSi, and Ca, RE-FeSi alloys, Table 1). W_3 chill wedge samples (ASTM A 367, 19 mm × 38 mm × 101 mm, 3.5 mm cooling modulus, weight 0.19 kg), plate samples (4.5 mm thickness), and round bar samples (25 mm diameter) are gated off the inoculation reaction chambers. A furan resin (3.0 wt.%) and P-Toluol Sulphonic Acid (PTSA as hardener) (6.53 wt.%S content and 1.5 wt.% addition) bonded silica sand (95.5 wt.%) (FRS-PTSA) molding system is used (thermal diffusivity 71 W S^{1/2}/m²K).

Table 1. Treatment Alloys (wt.%).

Role	Type	Si	Ca	Al	Ba	TRE *	Mg	Fe
Nodulizer	FeSiCaMgRE	44.7	1.0	0.91	0.04	0.26	5.99	Bal
	Ca-FeSi	73.8	1.02	0.77	-	-	-	Bal
Inoculant	Ca,Ba-FeSi	72.6	0.94	0.96	1.68	-	-	Bal
	Ca,RE-FeSi	73.5	0.87	0.83	-	1.86	0.06	Bal

* TRE total rare earth elements.

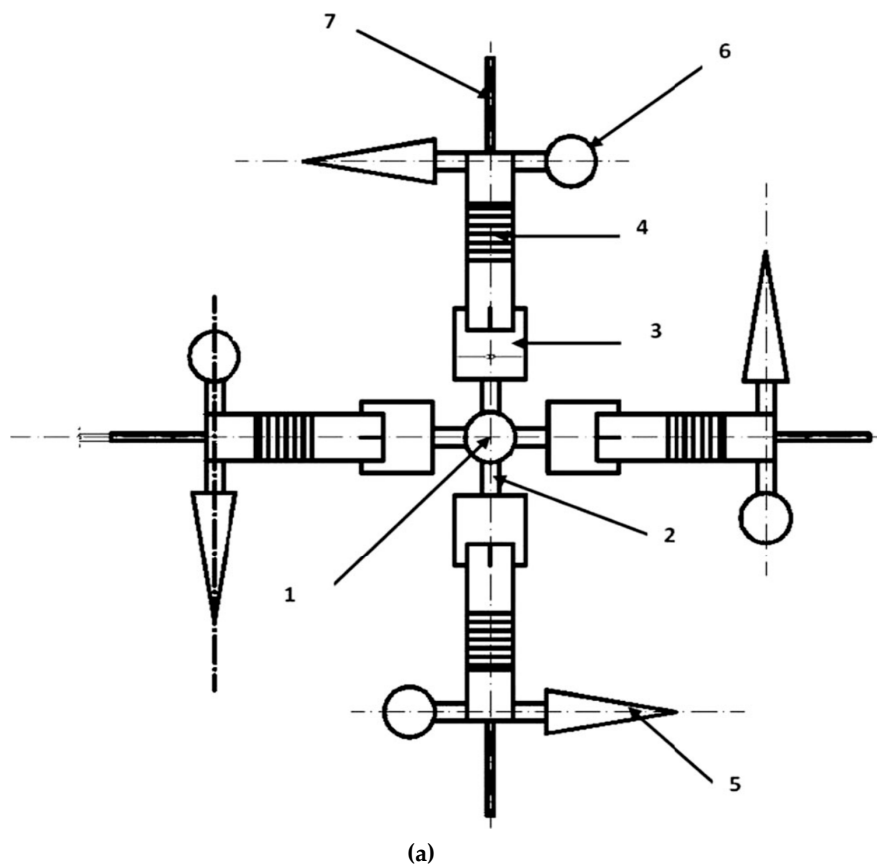
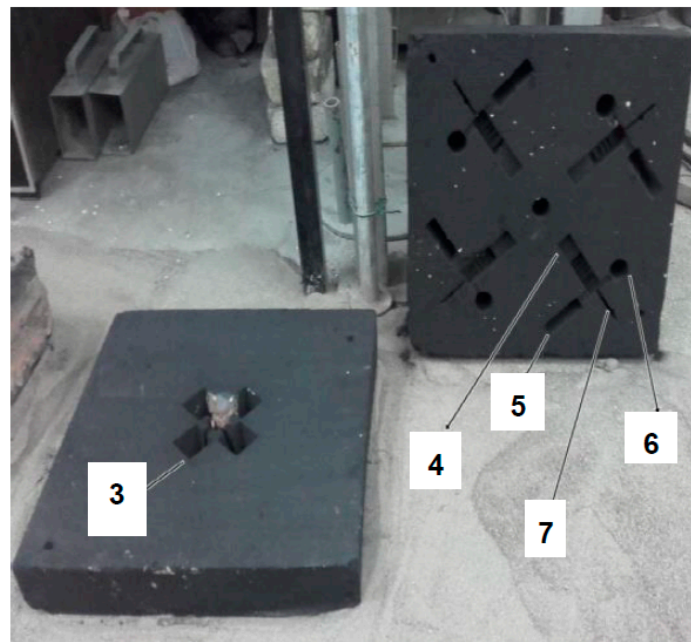


Figure 1. Cont.



(b)

Figure 1. In the mold inoculation pattern for four-work-position (1—Down sprue; 2—Gate; 3—Reaction chamber; 4—Runner; 5—Wedge sample; 6—Cylindrical bar; 7—Flat plate). (a) view on the four-work-position of supplied Mg-treated iron simultaneously to four separate reaction test chambers and samples; (b) view on the upper and lower moulds.

A SPECTROLAB high-end spectrometer (Sylmar, CA, USA) with hybrid optic (photomultiplier tubes (PMT) and CCD (Spectroscopic Charge Coupled Device detection system) detectors simultaneously) is used for a high precision metal analysis. The instrument achieves detection limits below 1 mg/Kg. The graphite characteristics are evaluated with Automatic Image Analysis (OMNIMET ENTERPRISE (Lake Bluff, IL, USA) and analySIS[®] FIVE Digital Imaging Solutions software).

3. Results and Discussion

3.1. Chemical Composition

Table 2 and Figure 2 show the chemical composition of the thin plate samples (Figure 1, position 7, thin samples) for un-inoculated and different inoculated Mg-treated cast irons. The rigid experimental procedure controls the produced narrow chemistry ranges for the most important elements, which included base chemistry elements (C, Si, Mn, P), nodularizing elements (Mg, Ce, La), and minor elements with possible contribution in graphite nucleation (Ca, Al, Zr, Ti, N), that affect carbide/pearlite formation (Ni, Cu, V, W, Bi, Cr, Mo, Co, Nb, Sn, Sb), and graphite degeneration (Pb, As, Bi). All these elements resulted from charge materials, and treatment alloys could influence final structure the characteristics [15]. Three control factors are considered: carbon equivalent (CE, Equation (1)), pearlite promotion factor (Px, Equation (2)) [16], and anti-nodularising factor (K, Equation (3)) [16].

$$CE = \%C + 0.3 (\%Si + \%P) - 0.03\%Mn + 0.4\%S \quad (1)$$

$$Px = 3.0 (\%Mn) - 2.65 (\%Si - 2.0) + 7.75 (\%Cu) + 90 (\%Sn) + 357 (\%Pb) + 333 (\%Bi) + 21.1 (\%As) + 9.60 (\%Cr) + 71.7 (\%Sb) \quad (2)$$

$$K = 4.4 (\%Ti) + 2.0 (\%Sn) + 5.0 (\%Sb) + 290 (\%Pb) + 370 (\%Bi) + 1.6 (\%Al) \quad (3)$$

For 3.27–3.35%C and 4.34–4.58%Si, the test cast irons are in a hypereutectic position (CE = 4.64–4.68%), with low manganese (0.20–0.25%Mn) and 0.040–0.043%P content. The nodularizing elements are represented by 0.032–0.036%Mg_{res}, 0.0004–0.0221%Ce_{res}, 0.0061–0.043%La_{res}, and 0.0038–0.024%Ca_{res}, with visible effects of the inoculation system. Without residual magnesium content affectation, inoculation will determine the content of Ca, Ce, and La. The lowest contents of Ca, Ce, and La resulted in un-inoculated iron. All these elements increased by inoculation, with maximum Ca content in Ca-FeSi treatment and Ce and La in Ca, RE-FeSi inoculated irons. The analysis system does not allow to determine Ba residual content.

The content of minor elements is typical for commercial cast irons, with the presence of some residual elements, tolerated in high silicon ductile irons, according to recent research works [8,9,17]. Two major effects of minor elements are considered on the cast iron structure in conjunction with final chemistry: pearlite promotion ($P_x = 2.4\text{--}3.0$) and anti-nodularizing effect ($K = 1.5\text{--}2.5$). Generally, rare earth elements are beneficial when $K < 1.2$, and essential when $K > 1.2$ [18,19].

Table 2. Chemical composition of Mg-treated in Inoculated Cast Irons * (wt.%).

Iron	C	Si	Mn	Mg	Ce	La	Ca	Al	CE
UI	3.33	4.55	0.22	0.035	0.0004	0.0061	0.0038	0.0054	4.65
Ca	3.33	4.34	0.20	0.032	0.0083	0.0080	0.024	0.0056	4.64
Ca, Ba	3.27	4.58	0.25	0.036	0.0097	0.0078	0.0142	0.0058	4.66
Ca RE	3.35	4.40	0.23	0.032	0.0221	0.0430	0.0118	0.0055	4.68

* Others elements (wt.%): 0.0048–0.0067 Ti, 0.040–0.043 P, 0.050–0.056 Cr, 0.10–0.24 Ni, 0.17–0.21 Cu, 0.065–0.080 Mo, 0.015–0.016 Sn, 0.02–0.03 As, 0.04–0.05 Sb, 0.001–0.004 Bi, 0.001–0.0045 Pb, 0.013–0.017 Co, 0.004–0.013 Nb, 0.007–0.011 V, 0.05–0.08 W, 0.019–0.057 N, CE carbon equivalent.

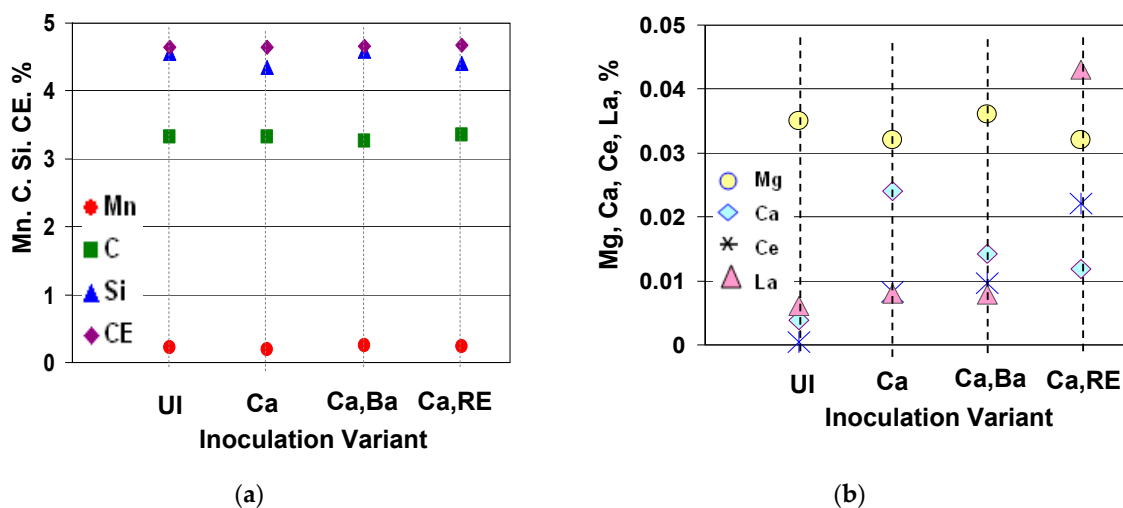


Figure 2. Base chemical composition (a) and nodularizing / inoculating elements (b) in final cast irons.

3.2. Graphite Characteristics

Structure analysis is performed on the wedge castings, from the apex up to the wedge base, at different wall thicknesses, as graphite and metal matrix characteristics. At the first approach, the graphite particles size (area), and count are evaluated at 3.5 and 10 mm wall thickness of the wedge casting in inoculated ductile cast irons (OMNIMET ENTERPRISE Image Analyzer, 70X magnification) (Figures 3–5). All the tested in-mold inoculated, ladle Mg treated cast irons are characterized by nodular (spherical) graphite morphology for both 3.5 and 10 mm wall thickness of W_3 wedge casting, ASTM A 367.

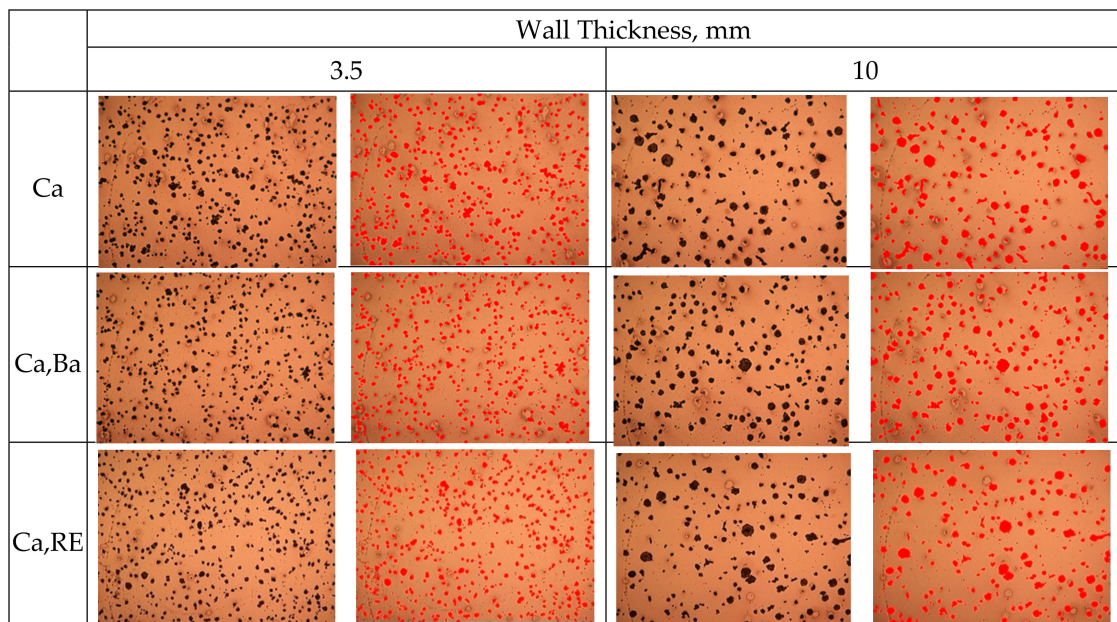


Figure 3. Micro-structures of inoculated (Ca/Ca, Ba/Ca, RE) ductile cast irons at 3.5 and 10 mm wedge casting thickness (70 X).

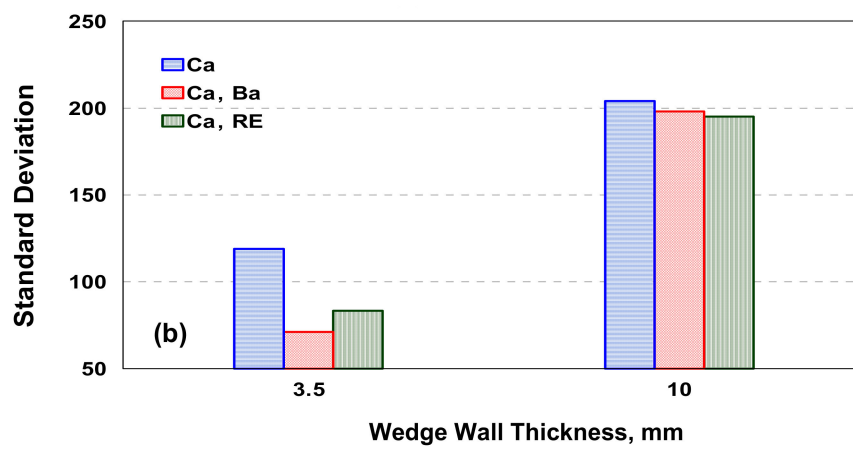
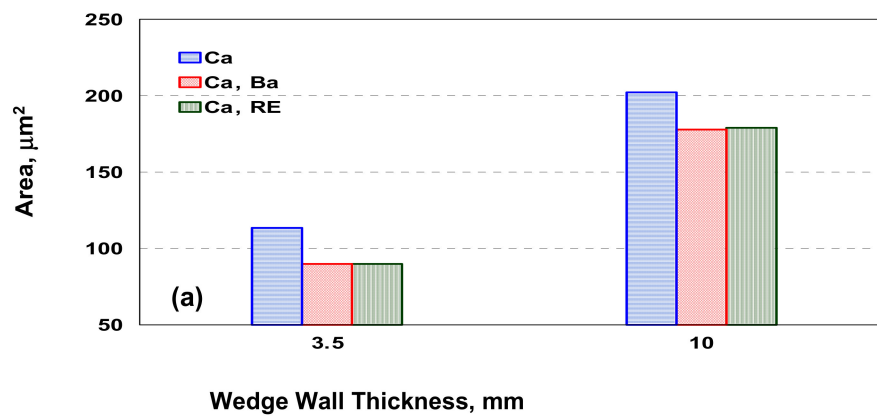


Figure 4. Cont.

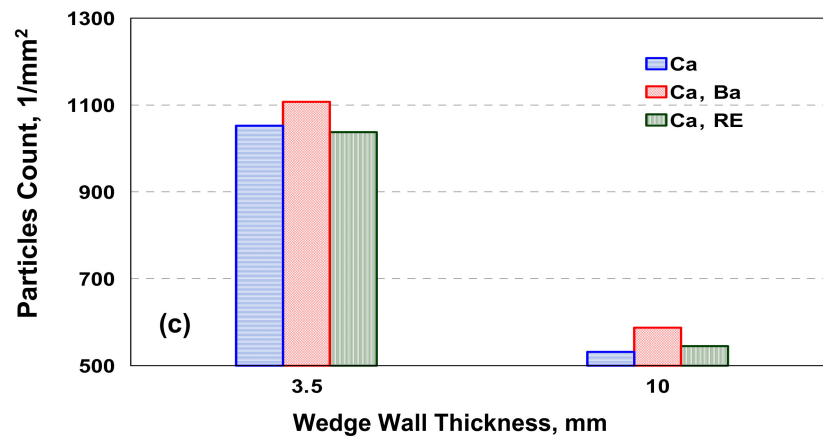


Figure 4. Average graphite particles characteristics. (a) area; (b) standard deviation in particles area values; (c) particle count.

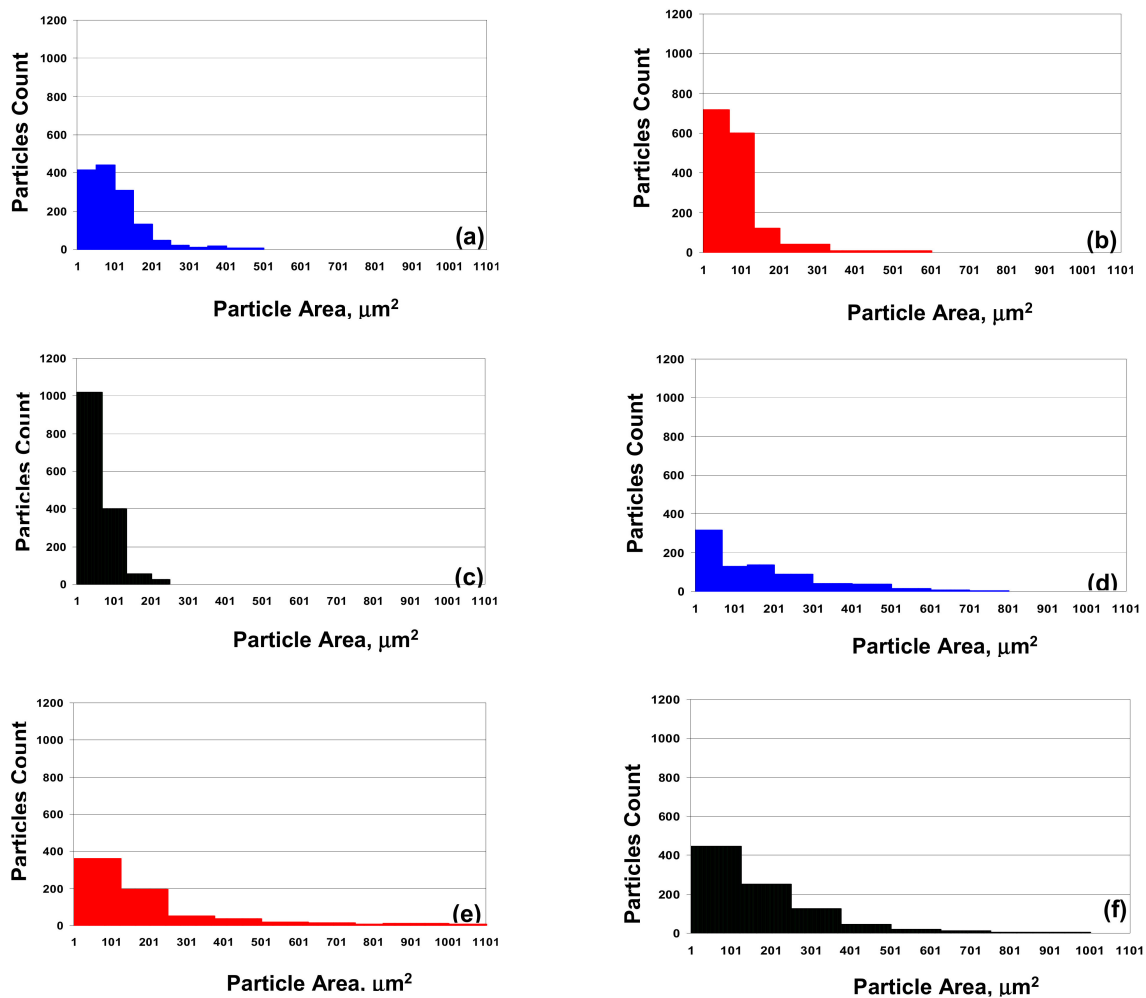


Figure 5. Size (area) distribution of graphite particles at 3.5 mm (a–c) and 10 mm (d–f) wall thickness in inoculated ductile cast irons (a,d—Ca; b,e—Ca,Ba; c,f—Ca,RE).

The cooling rate (wall thickness) has a visible effect on graphite phase parameters. Lower graphite particles area (Figure 4a), at lower standard deviation in graphite particles size (Figure 4b), expressed by standard deviation of the graphite particles area shown in Figure 4a, and higher graphite particles count (Figure 4c) characterizes the thin wall solidification (3.5 mm width of wedge casting), comparing

to 10 mm wall thickness. Regarding the size (area) distribution of the graphite particles, the wall thickness also has a visible influence, as Figure 5 shows. Higher solidification cooling rate, specifically for thin wall section (3.5 mm), higher the rate of very small particles, generally less than $200 \mu\text{m}^2$ area.

Inoculating elements represent the second influencing factor. Generally, it is a visible difference between Ca-FeSi inoculation, on the one hand, and Ca, Ba-FeSi and Ca, RE-FeSi inoculation, with visible vicinity, on the other hand. Especially for thin wall casting solidification conditions (3.5 mm thickness), where the complex inoculating alloys (including Ba or RE) lead to more than 1300 graphite particles at less than $100 \mu\text{m}^2$ area, comparing to less than 900 particles at this size, obtained by Ca-FeSi inoculation.

Generally, Ca-Ba and Ca-RE inoculated ductile cast irons are characterized by better parameters comparing to simple Ca inoculation, expressed by lower size, including standard deviation, and higher particles count, for both 3.5 and 10 mm thickness.

The Rare Earth bearing Ca-FeSi alloy does not appear to be superior compared to Ca, Ba-FeSi alloy, with better results for many parameters.

Recent experiments [4,5] find that the deviation using a sphere as reference of graphite particles is noticeably increased by silicon alloying. With more than 4%Si content, ductile irons are characterized by a medium quality graphite phase, with prevalent form V-ISO 945 graphite formation including cast irons that have been inoculated. As a characteristic of the graphite particles in these irons appears to be a larger perimeter. The sphericity shape factor (SSF, Equation (4)), which considers the real perimeter of a graphite particle, is recommended in Si alloyed ductile irons instead of the roundness shape factor (RSF, Equation (5)), involving maximum ferret of an analyzed particle, presently incorporated in the ISO 945 standard. If the minimum limit of SSF is increased, the graphite nodularity (Equation (6)) appears to go down, especially in Si-alloyed irons (Figure 6).

$$\text{SSF} = 4 \cdot \pi \cdot A_G / P_G^2 \quad (4)$$

$$\text{RSF} = 4 \cdot A_G / \pi \cdot F_{\max}^2 \quad (5)$$

$$\text{NG (SSF)} = 100 (\Sigma A_{\text{particles (SSF)}} / \Sigma A_{\text{all particles}}) \quad (6)$$

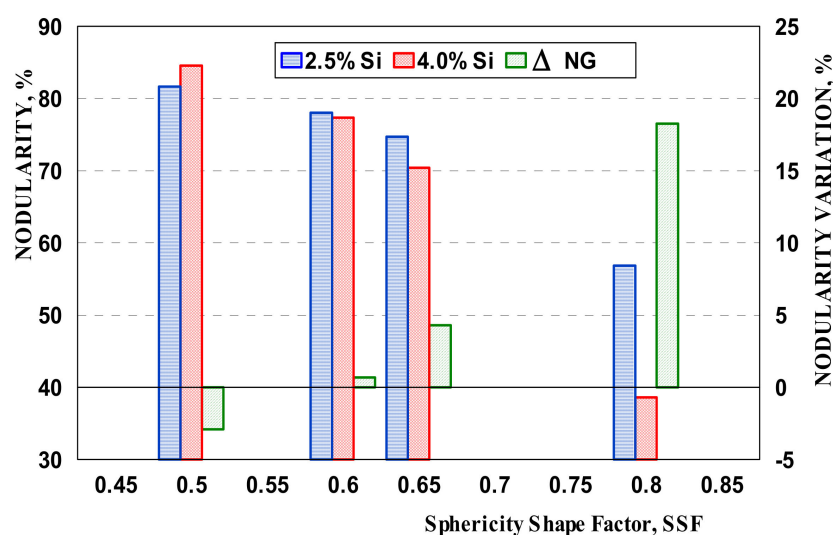


Figure 6. Influence of silicon (Si) content and minimum sphericity shape factor (SSF) on the graphite nodularity level and the difference (ΔNG) in graphite nodularity between 2.5%Si and 4%Si content ductile cast irons.

Where: A_G is the area of the graphite particle in question; P_G is the real perimeter of the graphite particle in question (the sum of the pixel distances along the closed boundary); F_{\max} is the maximum

ferret (length) of the object (graphite particle); $\Sigma A_{\text{particles}_{(\text{SSF})z}}$ —the sum of areas of graphite particles at a minimum considered SSF; $\Sigma A_{\text{all particles}}$ —the sum of areas of all of graphite particles.

As it was found that the inoculation could be an important factor to control the graphite phase characteristics in high silicon ductile cast iron, a second image analysis (analySIS® FIVE Digital Imaging Solutions software, particles greater than 6 μm) was applied, in order to put in evidence the effects of a larger wall thickness range, especially on the representative shape factors used in ductile iron characterization. Figure 7 shows the obtained microstructures, in Nital etching conditions, for 3, 6, 9, 12, and 15 mm wall thickness, W_3 wedge casting, ASTM A 367. For both un-inoculated and inoculated cast irons and for all of wedge sections (cooling rates), nodular (spheroidal) graphite resulted, as the major morphology. But the quality of the graphite phase depends on the three important influencing factors: inoculation, inoculant type, and cooling rate (wall thickness, the width of wedge casting). Different graphite shape factors are taken in consideration by Ruxanda and Stefanescu [20]. In the present paper, the typical parameters used in image analysis, are shown in Figure 8, and include:

- Maximum Ferret, F_{max} : longest distance measured between two parallel tangents on each side of the object of interest.
- Minimum Ferret, F_{min} : shortest distance measured between two parallel tangents on each side of the object of interest.
- Diameter circular (D_c): diameter of a circle having the same area with the object of interest.
- Real Perimeter (P_r): length of the outside boundary of the object of interest.
- Convex Perimeter (P_c): length of the convex outside boundary of the object of interest (a rubber band around all distances between two tangents).
- Area (A): area of the object of interest, minus the area of any holes.

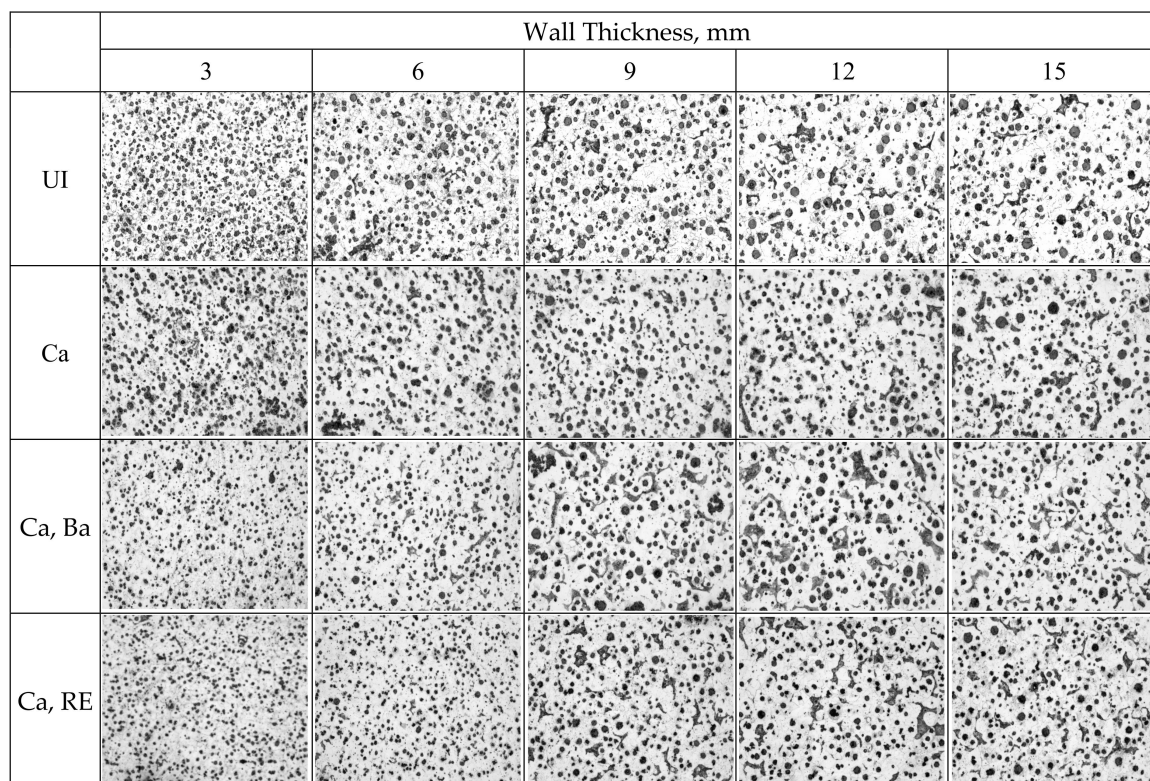


Figure 7. Micro-structures of un-inoculated and Ca/Ca, Ba/Ca, RE inoculated ductile cast irons, at different wall thickness (W_3 wedge casting, ASTM A 367) (Nital 2% etching).

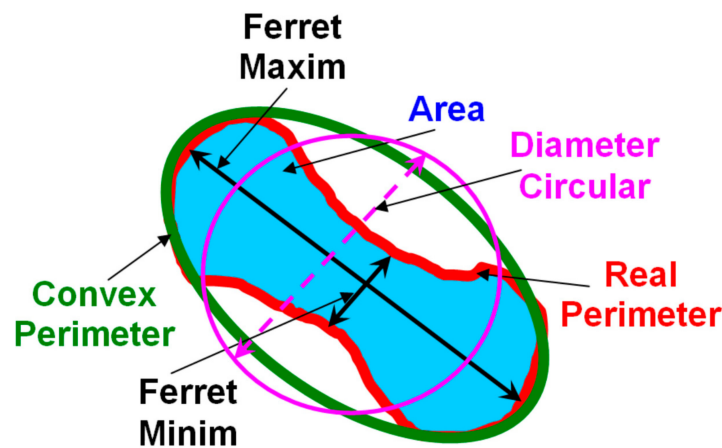


Figure 8. Considered Graphite Particle Parameters in image analysis.

Figure 9 summarizes the average values of size characteristics of graphite particles as influence of solidification cooling rate (higher wall thickness, lower cooling rate) for un-inoculated and Ca/Ca, Ba/Ca, RE-FeSi inoculated ductile cast irons. The average values of minimum (F_{\min}) size of graphite particles increase from 10 up to 16 μm , while the maximum (F_{\max}) particle size increases from 14 up to 23 μm , as the width of the wedge casting increases from 3 to 15 mm.

For 15 mm wedge width, close to the wedge base ($B = 19\text{mm}$), the end effect is present, as particles size decreased (higher cooling rate at the interface with the mold) (Figure 9a). A similar variation is also visible for the average area of graphite particles (Figure 9b). From 100–150 μm^2 at 3 mm section size area increasing up to the maximum level 200–275 μm^2 for 12 mm section size, followed by decreasing up to 165–230 μm^2 at 15 mm, as the end effect (Figure 9b).

The increasing of the casting wall thickness leads to increasing the level of graphite particles perimeter for both real and convex perimeter expressions. There is a visible difference between convex perimeter (Figure 9c) and real perimeter (Figure 9d), but this difference is lower at a higher solidification cooling rate (3 mm wall thickness and as the end effect). Generally, the real perimeter has not only higher values, compared to convex perimeter, but also a wider range of values.

Nodule count is strongly dependent on the section size and cooling rate, respectively (Figure 9e), with an evolution in opposite manner with particles size and area. More than 800 nodules per square mm are present at 3 mm section size, around 600 nodule count for 6 mm section size and with continuous decreasing for larger sections up to 400–600 nodule count.

Inoculation is also an influencing factor on the graphite particle size characteristics, but differently depending on the inoculating elements use, and the solidification cooling rate. In the present experimental conditions, and considering the non-inoculation as the reference, it can be seen that for 3 mm wall thickness, Ca-FeSi inoculation leads to the increasing of graphite particles size, area and their perimeter.

Contrary, Ca, Ba-FeSi and Ca, RE-FeSi inoculation decreases the average level of these parameters compared with un-inoculated ductile cast irons, with Ca, Ba-FeSi treatment having the strongest effect: the smallest particles as length, area, and perimeter (convex and real).

With the increasing of the wedge section size (6–15 mm), positions of Ca-FeSi (above un-inoculation points) and Ca, Ba-FeSi (below un-inoculation points) remain at the same. The rare earth bearing FeSi inoculation has a peculiar behavior: for the lowest length, area, and convex perimeter, graphite particles are characterized by a higher real perimeter.

Nodule count appears to be less influenced by inoculation and inoculating elements, as obtained values are included in a more restricted range for all of the section sizes, compared with other considered parameters of graphite (Figure 9e). The positive effect of inoculation in nodule count increasing appears to be visible for more than the 3 mm section size.

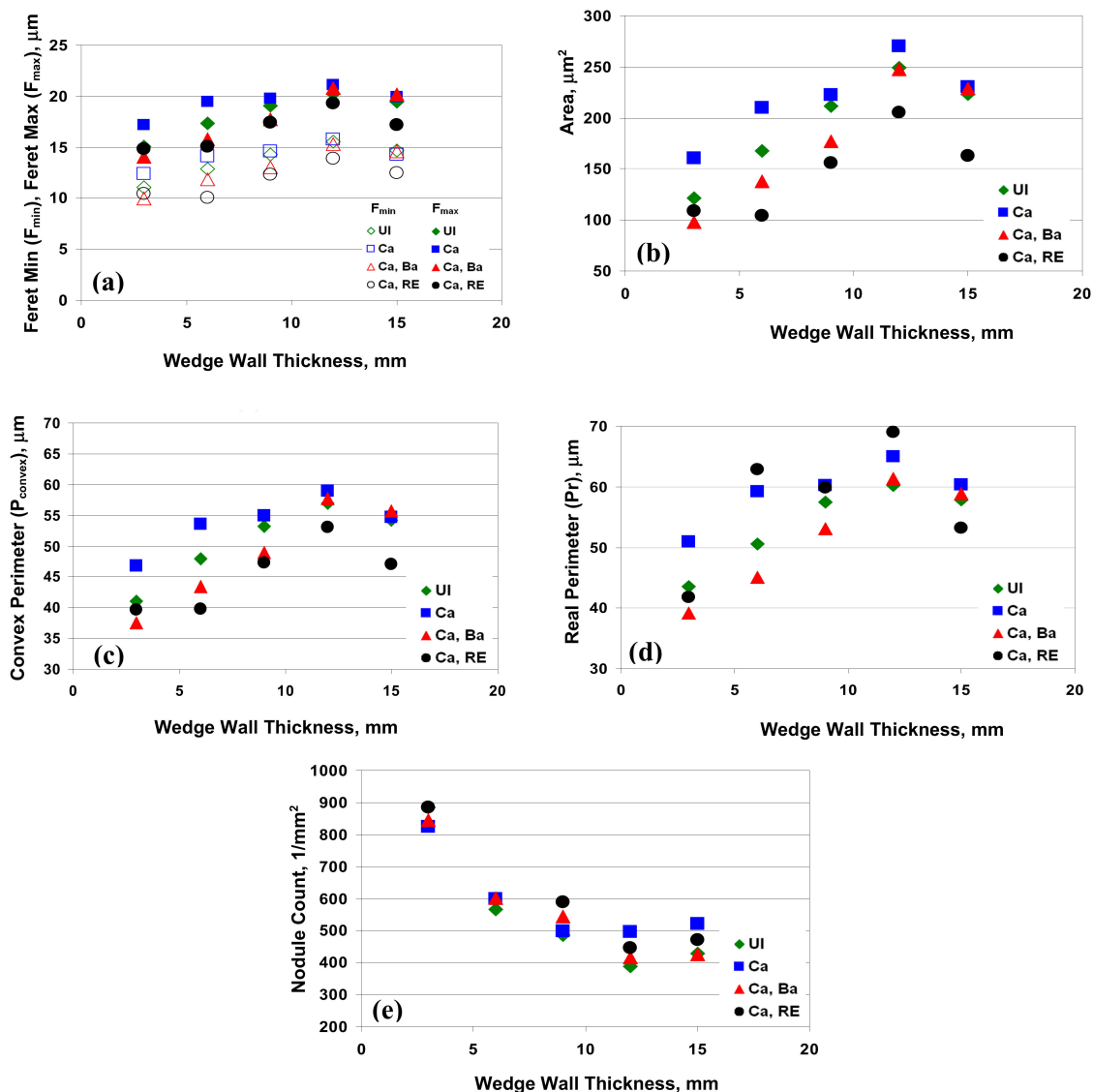


Figure 9. Influence of the wedge section size and inoculation on the average values of Minimum and Maximum Ferret (a), Area (b), Convex Perimeter (c), Real Perimeter (d), and Nodule count (e).

The graphs in Figure 10 show the representative graphite shape factors evolution as an effect of wedge section size and inoculation. Circularity (0.7–0.8), as a simple graphite shape factor, and expressed by the ratio between the diameter of a circle (D_C) having the same area with the graphite particle (A_C), and the maximum of its size (F_{max}), does not appear to be visibly influenced by the section size or cooling rate, respectively. Generally, inoculation leads to decreased values of this parameter, restricted for Ca and Ca,Ba inoculation, but more accentuated for Ca,RE inoculation.

Roundness Shape Factor (see Equation (5)) considers the area (A_C), and the maximum size (F_{max}) of graphite particles and it is usually used to evaluate the graphite nodularity in ductile cast irons [21,22]. In the present experiments, a general 0.6–0.8 range is obtained for this parameter, which is specific for slightly irregular spheroidal graphite morphology (Type V, ISO 945), as shown in Figure 11 [5], obtained on the base of 11 [21,22].

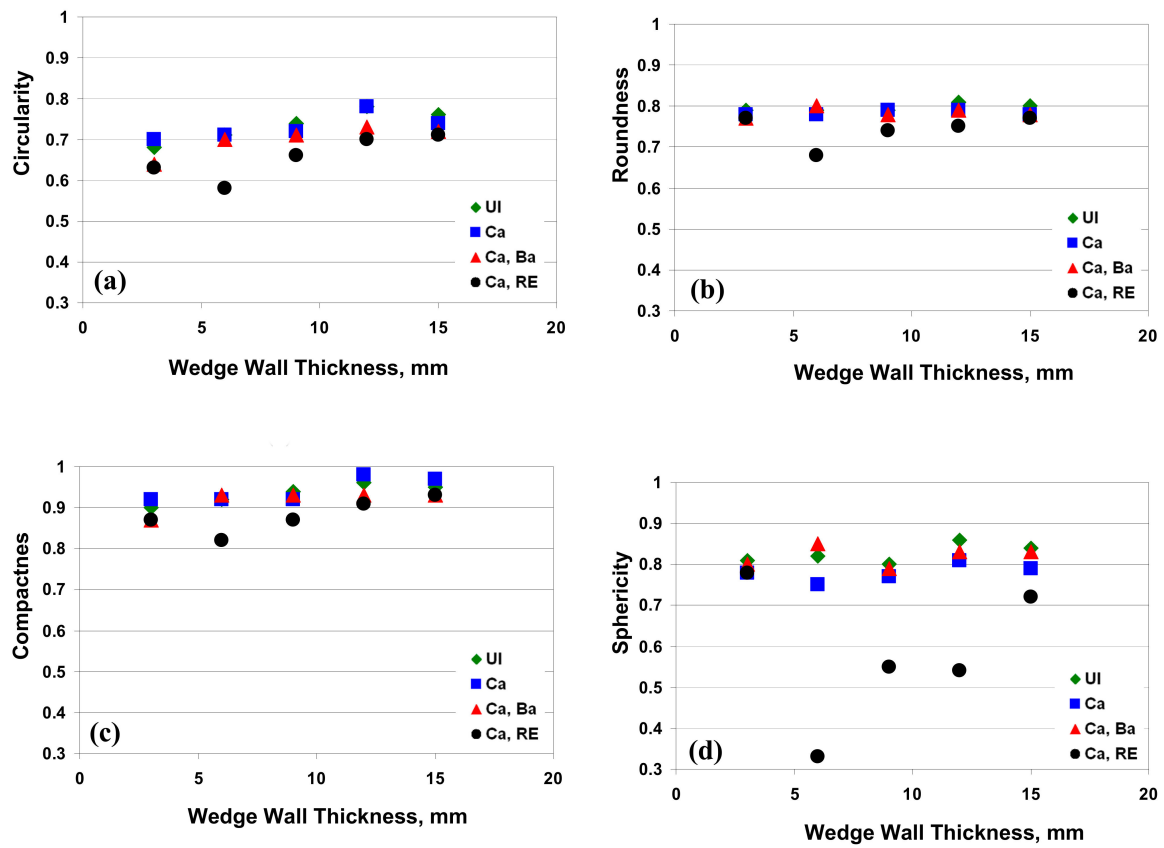


Figure 10. Graphite shape factors. (a) Circularity; (b) Roundness; (c) Compactness; (d) Sphericity.

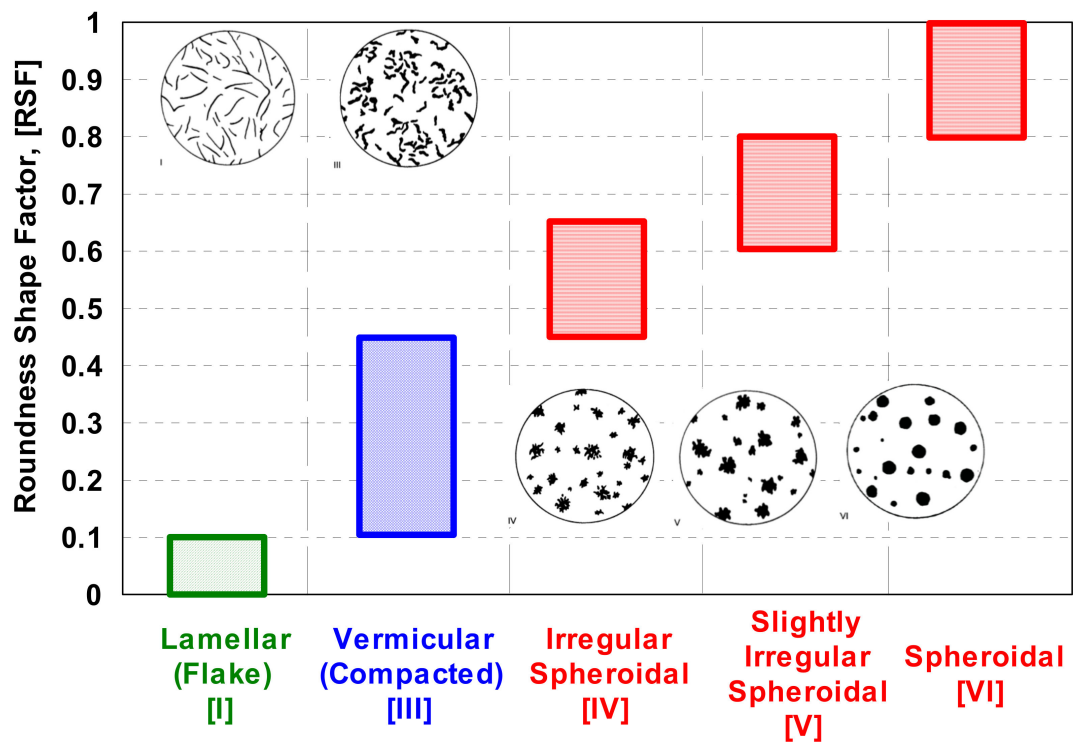


Figure 11. Representative graphite forms (ISO 945) characterized by Roundness Shape Factor (RSF).

In the tested casting wall thicknesses range (3–15 mm), an increasing tendency of this parameter is found, from 0.6–0.7 (3–6 mm) up to 0.7–0.8 (12–15 mm) range. The lowest roundness values characterize Ca, RE-FeSi inoculated ductile cast irons.

Another two shape factors consider the perimeter of graphite particles, Compactness concerning convex perimeter and Sphericity concerning real perimeter (see Figure 8). According to Figure 9c,d, the real perimeter is larger than the convex perimeter, their difference increasing with casting section size increasing. Compactness Shape Factor, mainly more than 0.85 level, has a slightly increasing tendency with section size increasing, with Ca, RE-FeSi inoculation values at the lowest level.

The larger real perimeter, the lower values for the Sphericity Shape Factor (less than 0.85), with the same large range distribution for more than 3 mm section size, like the one obtained for real perimeter. As rare earth bearing alloy inoculation produces graphite nodules with high real perimeter, the sphericity shape factor has not only the lowest values, but also the highest dispersion of these values (0.33–0.78), compared with 0.75–0.85 for other tested variants (Ca, Ba-FeSi better than Ca-FeSi inoculation).

3.3. Metal Matrix Characteristics

Mainly ferritic structures characterize all of the tested cast irons. Generally, inoculation leads to an increasing ferrite amount. It is found that the nodule count, higher for inoculated ductile cast irons solidified in thinner wall casting (more than 800 nodules per square mm) (Figure 9e), favors the highest ferrite amount (more than 99% ferrite in 3 mm thickness). The increasing of the wall thickness leads to decreasing the nodule count (Figure 9e) and the eutectic cells count, respectively, favoring inter-cells segregation. As a result, a small amount of pearlite is formed, less than 5% for 6 mm, 5–7% for 9 mm, and 4–10% for 12 mm casting thickness. It is found that Si-alloyed ductile cast irons tolerate the presence of minor elements at a higher level compared to conventional ductile irons, as promoters of pearlite ($P_x = 2.4\text{--}3.0$) and/or carbides, inclusively in thin wall solidification conditions.

4. Conclusions

- For relatively constant Mg_{res} level, Ca, Ce, and La content increases by inoculation, with maximum Ca content in Ca-FeSi treatment and Ce and La in Ca, RE-FeSi inoculated irons. The analysis system does not allow to determine Ba residual content.
- Ca-FeSi inoculation leads to increasing the graphite particles size, area and perimeter, while Ca, Ba-FeSi and Ca, RE-FeSi decrease the average level of these parameters, with Ca, Ba-FeSi treatment at the strongest effect: the smallest particles as length, area, and perimeter (convex and real) at 3 mm wall thickness.
- With the increasing of the wedge section size more than 3 mm, Ca-FeSi and Ca, Ba-FeSi act in the same way, while the RE-bearing FeSi inoculation has a peculiar behavior: for the lowest length, area, and convex perimeter, graphite particles are characterized by a higher real perimeter.
- Generally, the real perimeter has not only higher values, compared to convex perimeter, but also a wider range of values, but this difference is lower at higher solidification cooling rate.
- Nodule count appears to be less influenced by inoculation and inoculating elements than by section size (cooling rate) variation, with a more restricted values range compared with other parameters.
- Roundness Shape Factor (including A_G and F_{max}) at 0.6–0.8 level illustrates the common formation of slightly irregular spheroidal graphite morphology (Type V, ISO 945), more accentuated thin wall thicknesses (less than 0.7 for less than 10 mm section size), with Ca, RE-FeSi inoculation at the lowest values, for entire section size range.
- By involving the real perimeter, higher than convex perimeter, Sphericity Shape Factor (0.33–0.78) is lower than Compactness Shape Factor (0.75–0.85), with the same large range distribution for more than 3 mm section size, like the one obtained for real perimeter. Ca, Ba-FeSi is better than Ca-FeSi inoculation, while Ca, RE-FeSi drastically decreases this graphite shape factor.

- In the present experimental conditions, for high Si-ductile iron solidified in thin wall castings, Ca, Ba-FeSi inoculation appears to be better than simple Ca-FeSi for most of the graphite parameters improving, while Ca, RE-FeSi has the lowest beneficial effect, especially as negatively affecting the compactness degree of graphite particles.
- As Ca, Ba-FeSi shows the best inoculant, expressed by graphite particles shape factors improving, it can be expected that Ca, Ba-FeSi inoculant will result in the best strength to weight ratio.
- A two-step liquid treatment, as ladle treatment using RE-bearing FeSiCaMg master alloy and in-mold inoculation using Ca, Ba-FeSi alloy appears to be a solution to improve graphite parameters for high-Si ductile irons solidified in thin wall castings.
- More experiments are necessary to elucidate the mechanism of the specific action of the inoculating elements, such as Ca, Ba, and RE on the nodular graphite formation in high silicon ductile cast irons.

Author Contributions: Conceptualization, I.R., E.S., S.S., N.R.P. and M.C.; methodology, I.R., E.S., S.S., N.R.P. and M.C.; validation, I.R., E.S., S.S., N.R.P. and M.C.; investigation, I.R., E.S., S.S., N.R.P. and M.C.; writing—original draft preparation, I.R., E.S., S.S., N.R.P. and M.C.; writing—review and editing, I.R., E.S., S.S., N.R.P. and M.C.; supervision, I.R., E.S., S.S., N.R.P. and M.C. All authors have read and agreed to the published version of the manuscript.

Funding: This research received no external funding.

Conflicts of Interest: The authors declare no conflict of interest.

References

1. Dawson, S. Automotive Powertrain Trends and the Market Opportunity for Cast Iron. In Proceedings of the 2nd Carl Loper Cast Iron Symposium, Bilbao, Spain, 30 September–1 October 2019.
2. Fraś, E.; Górný, M.; Kapturkiewicz, W. Thin Wall Ductile Iron Castings: Technological Aspects. *Arch. Foundry Eng.* **2013**, *13*, 23–28. [\[CrossRef\]](#)
3. Frás, E.; Górný, M.; Lopez, H. Thin Wall Ductile Iron Castings as Substitutes for Aluminum Alloy Castings. *Arch. Metall. Mat.* **2014**, *59*, 459–465. [\[CrossRef\]](#)
4. Stan, S.; Riposan, I.; Chisamera, M.; Barstow, M. Solidification pattern of silicon alloyed ductile cast irons. In Proceedings of the 122nd AFS Metalcasting Congress, Fort Worth, TX, USA, 3–5 April 2018; pp. 18–22.
5. Stan, S.; Riposan, I.; Chisamera, M.; Stan, I. Solidification characteristics of silicon alloyed ductile cast irons. *J. Mater. Eng. Perform.* **2019**, *28*, 278–286. [\[CrossRef\]](#)
6. Bauer, B.; Mihalic Pokopec, I.; Petric, M.; Mrvar, P. Effect of Si and Ni addition on graphite morphology in heavy section spheroidal graphite iron parts. *Mater. Sci. Forum* **2018**, *925*, 70–77. [\[CrossRef\]](#)
7. Larranaga, P.; Asenjo, I.; Sertucha, J.; Suarez, R.; Ferrer, I.; Lacaze, J. Effect of antimony and cerium on the formation of chunky graphite during solidification of heavy-section castings of near-eutectic spheroidal graphite irons. *Metall. Mater. Trans. A* **2009**, *40*, 654–661. [\[CrossRef\]](#)
8. Stets, W.; Loblich, H.; Gassner, G.; Schumacher, P. Solution strengthened ferritic ductile cast iron according DIN EN1563:2012—properties, production and application. In Proceedings of the “Keith Millis” Symposium on Ductile Iron, Nashville, TN, USA, 15–17 October 2013; pp. 283–292.
9. Dommaaschk, C. Chances and limits of High silicon ductile iron. In Proceedings of the WFO Technical Forum, Emperors Palace, Kempton Park, Gauteng, South Africa, 14–17 March 2017.
10. Baer, W. Chunky Graphite in Ferritic Spheroidal Graphite Cast Iron: Formation, Prevention, Characterization, Impact on Properties: An Overview. *Int. J. Met.* **2020**, *14*, 454–488. [\[CrossRef\]](#)
11. Gonzalez-Martinez, R.; de la Torre, U.; Lacaze, J.; Sertucha, J. Effects of high silicon contents on graphite morphology and room temperature mechanical properties of as-cast ferritic ductile cast irons. Part I—Microstructure. *Mater. Sci. Eng. A* **2018**, *712*, 794–802. [\[CrossRef\]](#)
12. Gonzalez-Martinez, R.; de la Torre, U.; Ebel, A.; Lacaze, J.; Sertucha, J. Effects of high silicon contents on graphite morphology and room temperature mechanical properties of as-cast ferritic ductile cast irons. Part II—Mechanical properties. *Mater. Sci. Eng. A* **2018**, *712*, 803–811. [\[CrossRef\]](#)
13. Stefanescu, D.M.; Ruxanda, R.; Dix, L.P. The metallurgy and tensile mechanical properties of thin wallspheroidal graphite irons. *Int. J. Cast Met. Res.* **2003**, *16*, 319–324. [\[CrossRef\]](#)

14. Riposan, I.; Skaland, T. Modification and inoculation of cast iron. In *Cast Iron Science and Technology Handbook*; Stefanescu, D.M., Ed.; American Society of Materials: Materials Park, OH, USA, 2017; pp. 160–176.
15. Bai, J.-X. Selection of raw materials and control of trace elements for production of high-quality SG iron. *China Foundry* **2019**, *16*, 79–87. [[CrossRef](#)]
16. Thielemann, T. Zur Wirkung van Spuren elementen in Gusseisen mit Kugel graphit. *Giessereitechnik* **1970**, *16*, 16–24.
17. Hammersberg, P.; Hamberg, K.; Bjorkegren, L.E.; Lindkvist, J.; Borgstrom, H. Sensitivity to Variation of Tensile Properties of High Silicon Ductile Iron. In Proceedings of the 11th International Symposium On the Science and Processing of Cast Iron (SPCI-XI), Jonkoping, Sweden, 4–7 September 2017; p. 53.
18. Riposan, I.; Chisamera, M.; Stan, S. Influencing Factors on the As-cast and Heat Treated 400-18 SG Iron Grade Characteristics. *China Foundry* **2007**, *4*, 300–303.
19. Riposan, I.; Chisamera, M.; Uta, V.; Stan, S.; Naro, R.; Williams, D. The importance of rare earth contribution from nodulizing alloys and their subsequent effect on the inoculation of ductile iron. *Int. J. Met.* **2014**, *8*, 65–80. [[CrossRef](#)]
20. Ruxanda, R.; Stefanescu, D.M. GraphiteShape Characterization in Cast Iron. From Visual Estimation to Fractal Dimension. *Int. J. Cast Met. Res.* **2002**, *14*, 207–216. [[CrossRef](#)]
21. *ISO 945-4: Microstructure of Cast Irons-Part 4: Determination of Nodularity in Spheroidal Graphite Cast Irons*; International Standard Organization (ISO): Geneva, Switzerland, 2015.
22. GB/T 9441-2009. *Metallographic Test for Evaluation of Spheroidal Graphite Cast Iron*. (National Standard of the People's Republic of China); Standardization Administration of China: Beijing, China, 2009.



© 2020 by the authors. Licensee MDPI, Basel, Switzerland. This article is an open access article distributed under the terms and conditions of the Creative Commons Attribution (CC BY) license (<http://creativecommons.org/licenses/by/4.0/>).